THE DEUTERIUM CHEMISTRY OF THE EARLY UNIVERSE

P. C. STANCIL,[1,2] S. LEPP,[3] AND A. DALGARNO[4]

ABSTRACT

The chemistry of deuterium, as well as that of hydrogen and helium, in the postrecombination era of the expanding early universe is presented. A thorough survey of all potentially important gas-phase reactions involving the primordial elements produced in the Big Bang, with a particular emphasis on deuterium, is given. The reaction set, consisting of 144 processes, is used in a nonequilibrium chemistry model to follow the production of primordial molecules in the postrecombination era. It is found that significant deuterium fractionation occurs for HD^+, HD, and H_2D^+, while the abundance of D^+ is reduced compared to the proton abundance. Even with the enhanced fractionation of H_2D^+, its abundance is predicted to be too small to cause any interesting cosmological consequences, such as possible attenuation of spatial anisotropies in the cosmic background radiation field, detections of the epochs of reionization and reheating, or constraints on the primordial deuterium abundance. HD, being the second most abundant primordial molecule after H_2, may play a role in subsequent structure formation because of its cooling radiation.

Subject headings: cosmic microwave background — early universe — molecular processes — nuclear reactions, nucleosynthesis, abundances

1. INTRODUCTION

Deuterium at early epochs has attracted renewed interest as a consequence of the controversy regarding its observed fractional abundance in high-redshift Lyα clouds (Songaila et al. 1994; Carswell et al. 1994, 1996; Tytler, Fan, & Burles 1996; Burles & Tytler 1996). Further, Dubrovich (1993) has suggested that primordial H_2D^+, which has a significant dipole moment (~ 0.6 Debye), may be detected through its effect on the cosmic background radiation (CBR) field. If H_2D^+ is sufficiently abundant, Thomson scattering of CBR photons may provide a partial attenuation of CBR spatial anisotropies. Finally, there remains optimism that HD may be observed in the first collapsing objects and that it may play a role in formation of these objects via its radiative cooling. It is important, therefore, to ensure that the deuterium chemistry is soundly established.

Early universe chemistry has been previously investigated by Lepp & Shull (1983); Dalgarno & Lepp (1987); Latter (1989); Puy et al. (1993); Palla, Galli, & Silk (1995); Stancil, Lepp, & Dalgarno (1996); Abel et al. (1997); Bougleux & Galli (1997); and Galli & Palla (1998; hereafter GP), while Dalgarno & Lepp (1984), Pineau des Forêts, Roueff, & Flower (1989), Rodgers & Millar (1996), and others have discussed the chemistry of deuterium in the interstellar medium. We improve upon the previous work by constructing a comprehensive chemistry. Fractional abundances of e^-, H, H^+, H^-, D, D^+, D^-, He, He^+, Li, Li^+, Li^-, H_2, H_2^+, HD, HD^+, He_2^+, HeH^+, HeD^+, H_3^+, H_2D^+, LiH, and LiH^+ are calculated for redshifts z between 4000 and 10 in an expanding universe. 144 reactions are included with their rate coefficients taken from the most recent theoretical or experimental evaluations. Enhancements to molecule for-

mation through stimulated radiative association are included. The recombination-era gas-phase chemistry is discussed in § 2, while § 3 presents the adopted cosmological models. The results of atomic and molecular abundance calculations are presented in § 4 with their cosmological implications discussed in § 5.

2. EARLY UNIVERSE CHEMISTRY

After the epoch of nucleosynthesis, the universe was saturated with a high-temperature CBR field delaying both electronic and chemical bonding. As the universe expanded, it cooled, allowing for the formation in chronological order of Li^{2+}, He^+, Li^+, He, D, H, and Li by radiative recombination and D^-, H^-, and Li^- through radiative attachment. With the formation of neutral helium, the universe was poised for the appearance of one of the first chemical bonds in He_2^+ by the radiative association process (T1.98)[5]

$$He^+ + He \rightarrow He_2^+ + v . \tag{1}$$
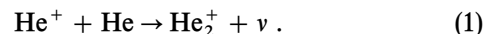
Its abundance was severely limited by the photodissociation reaction (T1.99) and dissociative recombination (T1.100). The formation of He_2^+ was later hindered by the removal of He^+ by radiative recombination (T1.17). As such, while it was the first molecule to form, it never reached sufficient abundances to be of interest. $LiHe^+$ was also produced and destroyed through similar processes (Dalgarno & Fox 1994) but was even less abundant.

Following the production of neutral He, the molecular ions HeH^+ and HeD^+ were formed by the radiative association processes (T1.37)

$$He + H^+ \rightarrow HeH^+ + v \tag{2}$$
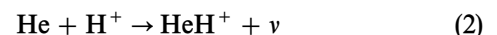
and (T1.70), respectively. Because these reactions proceed within the ground electronic state of the molecule, the frequency v of the emitted radiation is comparable to that of CBR frequencies v_r. This suggests (V. K. Dubrovich 1996, private communication) that molecule formation could be

[1] Physics Division, Oak Ridge National Laboratory, P.O. Box 2008, Oak Ridge, TN 37831-6372; stancil@mail.phy.ornl.gov.
[2] Eugene P. Wigner Fellow.
[3] W. M. Keck Laboratory for Computational Physics, Department of Physics, University of Nevada, Las Vegas, NV 89154-4002; lepp@physics.unlv.edu.
[4] Harvard-Smithsonian Center for Astrophysics, 60 Garden Street, Cambridge, MA 02138; adalgarno@cfa.harvard.edu.

[5] The notation (T1.x) refers to process (x) of Table 1.

enhanced by the stimulated processes (T1.38)

$$\mathrm{He} + \mathrm{H}^+ + v_r \rightarrow \mathrm{HeH}^+ + v + v_r \qquad (3)$$
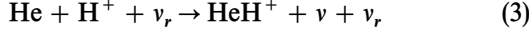
and (T1.71). The effect was investigated by Stancil & Dalgarno (1997a) and Zygelman, Stancil, & Dalgarno (1998) and found to only increase molecular abundances by $\sim 20\%$–30%.

With the appearance of neutral H and D, reactions (T1.40) and (T1.69) produce additional HeH^+ and HeD^+. The helium hydride ions are destroyed by photodissociation (T1.39) and (T1.72), by dissociative recombination (T1.43) and (T1.77), and by reactions with H (T1.41) and (T1.75). Electronic photodissociation reactions such as

$$\mathrm{HeH}^+ + v \rightarrow \mathrm{He}^+ + \mathrm{H} \qquad (4)$$
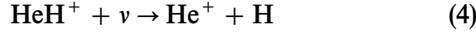
are not important, because UV radiation is insignificant until after the first stars are created. The molecular ion HeH^+ can also be formed by the reaction of vibrationally excited H_2^+ with He (T1.42):

$$\mathrm{H}_2^+(v \geq 2) + \mathrm{He} \rightarrow \mathrm{HeH}^+ + \mathrm{H} \ . \qquad (5)$$

As the universe cooled further, the stage was set for the beginning of chemistry with the formation of the first neutral molecules. Since dust grains had yet to form, H_2 could only be formed through the gas-phase H_2^+ and H^- sequences: radiative association (T1.27) followed by the charge exchange reaction (T1.31)
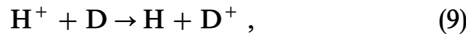
$$\mathrm{H}_2^+ + \mathrm{H} \rightarrow \mathrm{H}_2 + \mathrm{H}^+ \qquad (6)$$
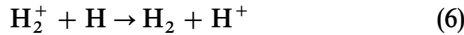
and radiative attachment (T1.3)

$$\mathrm{H} + e^- \rightarrow \mathrm{H}^- + v \ , \qquad (7)$$
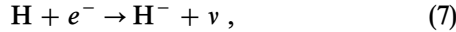
followed by associative detachment (T1.36)

$$\mathrm{H}^- + \mathrm{H} \rightarrow \mathrm{H}_2 + e^- \ . \qquad (8)$$
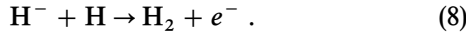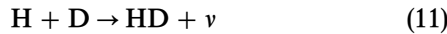
HD was formed by the similar reactions (T1.51), (T1.53), (T1.58), (T1.10), (T1.67), and (T1.68). The sequence (T1.8)

$$\mathrm{H}^+ + \mathrm{D} \rightarrow \mathrm{H} + \mathrm{D}^+ \ , \qquad (9)$$

followed by (T1.63)

$$\mathrm{H}_2 + \mathrm{D}^+ \rightarrow \mathrm{HD} + \mathrm{H}^+ \ , \qquad (10)$$
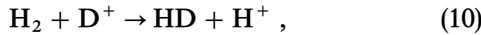
which is the major source of HD in diffuse interstellar clouds (Dalgarno, Weisheit, & Black 1973), may produce additional HD in the early universe, while the radiative association reaction (T1.61)

$$\mathrm{H} + \mathrm{D} \rightarrow \mathrm{HD} + v \qquad (11)$$

(Stancil & Dalgarno 1997b) gives only a minor contribution.

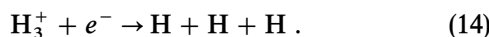H_3^+, an important ion in interstellar chemistry, is formed in the early universe by the hydrogen abstraction reaction (T1.44)
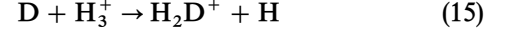
$$\mathrm{H}_2^+ + \mathrm{H}_2 \rightarrow \mathrm{H}_3^+ + \mathrm{H} \ , \qquad (12)$$
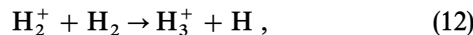
but it is readily removed via dissociative recombination (T1.48)

$$\mathrm{H}_3^+ + e^- \rightarrow \mathrm{H}_2 + \mathrm{H} \qquad (13)$$

and (T1.49)

$$\mathrm{H}_3^+ + e^- \rightarrow \mathrm{H} + \mathrm{H} + \mathrm{H} \ . \qquad (14)$$

Collisions with D (T1.87)

$$\mathrm{D} + \mathrm{H}_3^+ \rightarrow \mathrm{H}_2\mathrm{D}^+ + \mathrm{H} \qquad (15)$$

can deplete the H_3^+ abundance and form $\mathrm{H}_2\mathrm{D}^+$. The deuterated molecular ion $\mathrm{H}_2\mathrm{D}^+$ is also produced by (T1.86)

$$\mathrm{HD}^+ + \mathrm{H}_2 \rightarrow \mathrm{H}_2\mathrm{D}^+ + \mathrm{H} \qquad (16)$$

and (T1.88)

$$\mathrm{HD} + \mathrm{H}_2^+ \rightarrow \mathrm{H}_2\mathrm{D}^+ + \mathrm{H} \qquad (17)$$

and destroyed by dissociative recombination (T1.83)–(T1.85)

$$\mathrm{H}_2\mathrm{D}^+ + e^- \rightarrow \mathrm{H} + \mathrm{H} + \mathrm{D} \ , \qquad (18)$$

$$\mathrm{H}_2\mathrm{D}^+ + e^- \rightarrow \mathrm{H}_2 + \mathrm{D} \ , \qquad (19)$$

and

$$\mathrm{H}_2\mathrm{D}^+ + e^- \rightarrow \mathrm{HD} + \mathrm{H} \ . \qquad (20)$$
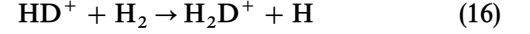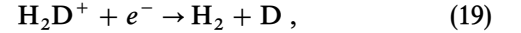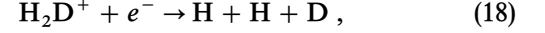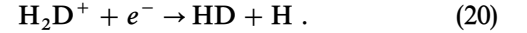
The presently adopted reaction rate coefficients $\alpha(T)$ are listed in Table 1. They are taken from the most recent calculations or experiments available; others are deduced from experimental or theoretical studies on related systems, while the remainder are estimates and are subject to considerable uncertainty. If no data exist for a reaction involving deuterium, we adopt a rate coefficient equal to the analogous hydrogen reaction but scaled by the ratio of the collision system reduced-mass μ, assuming the rate coefficients to have the form $\alpha(T) \propto T^m \propto 1/\mu^m$, where m is some power. The sources of the data are given in the table, and the reactions are generally listed for the exothermic direction.

3. COSMOLOGICAL MODELS

To estimate the particle abundances in the expanding universe, we take into account the chemical reactions listed in Table 1 and the lithium processes tabulated in Stancil et al. (1996)[6]. The corresponding chemical rate equations form a set of coupled stiff differential equations for the particle densities $n(x)$ of the form

$$\frac{dn(x)}{dt} = \alpha_{\mathrm{form}}(T_m)n(y)n(w) - \zeta_{\mathrm{dest}}(T_r)n(x) - \alpha_{\mathrm{dest}}(T_m)n(x)n(u) \ ,$$
$$(21)$$

which depend upon the total density and the temperature, and which must be integrated in time t. The photodestruction rate ζ_{dest} is obtained by detailed balance using the appropriate equilibrium constant and the corresponding formation rate α_{form}. Partition functions are taken from Irwin (1981), while the equilibrium constants are given by Sauval & Tatum (1994), except for HeH^+, which was taken from Gaur & Tripathi (1985).

For the recombination epoch we assume that the hydrogen density is given by

$$n_{\mathrm{H}} = 1.123 \times 10^{-5}(1 - Y)\Omega_b h^2(1 + z)^3 \ \mathrm{cm}^{-3} \qquad (22)$$

---

[6] See Stancil & Dalgarno (1997a, 1998) and Stancil & Zygelman (1996) for some improvements to the lithium chemistry. Additionally, the radiative association reaction $\mathrm{Li} + \mathrm{H} \rightarrow \mathrm{LiH} + v$ should have the form $3.74 \times 10^{-20}(T/300)^{0.11} \exp{(-T/2000)} \ \mathrm{cm}^3 \ \mathrm{s}^{-1}$ for $T < 380$ K, and the mutual neutralization reactions $\mathrm{Li}^+ + \mathrm{H}^- \rightarrow \mathrm{Li} + \mathrm{H}$ and $\mathrm{Li}^- + \mathrm{H}^+ \rightarrow \mathrm{Li} + \mathrm{H}$ are better represented by the fit $1.57 \times 10^{-7}(T/300)^{-0.49} \exp{(T/11800)} \ \mathrm{cm}^3 \ \mathrm{s}^{-1}$.

TABLE 1
Gas-Phase Reactions and Their Rate Coefficients

Reaction	a_1 (cm^3 s^{-1})	a_2	a_3 (K)	Notes
(1) $H^+ + e^- \rightarrow H + v$	3.6E−12[a]	−0.75	...	1
(2) $H + v \rightarrow H^+ + e^-$	...	...	...	2
(3) $H + e^- \rightarrow H^- + v$	3.0E−16	0.95	9320	3
(4) $H^- + v \rightarrow H + e^-$	...	...	...	2
(5) $H^+ + H^- \rightarrow H + H$	4.0E−8	−0.50	...	4
(6) $D^+ + e^- \rightarrow D + v$	3.6E−12	−0.75	...	1
(7) $D + v \rightarrow D^+ + e^-$	...	...	...	2
(8) $H^+ + D \rightarrow H + D^+$	1.0E−9	...	41[b]	5
(9) $D^+ + H \rightarrow D + H^+$	1.0E−9	...	...	5
(10) $D + e^- \rightarrow D^- + v$	3.0E−16	0.95	9320	6
(11) $D^- + v \rightarrow D + e^-$	...	...	...	2
(12) $D^+ + D^- \rightarrow D + D$	5.7E−8	−0.50	...	7
(13) $D^+ + H^- \rightarrow D + H$	4.6E−8	−0.50	...	7
(14) $H^+ + D^- \rightarrow D + H$	4.6E−8	−0.50	...	7
(15) $H^- + D \rightarrow H + D^-$	6.4E−9	0.41	...	8
(16) $D^- + H \rightarrow D + H^-$	6.4E−9	0.41	...	8
(17) $He^+ + e^- \rightarrow He + v$	4.51E−12	−0.67	...	9
(18) $He + v \rightarrow He^+ + e^-$	...	...	...	2
(19) $He^+ + H \rightarrow He + H^+ + v$	1.20E−15	0.25	...	10
(20) $He^+ + H^- \rightarrow He + H$	2.32E−7	−0.52	−22400	11
(21) $He^+ + D \rightarrow He + D^+ + v$	1.1E−15	0.25	...	7
(22) $He^+ + D^- \rightarrow He + D$	3.03E−7	−0.52	−22400	7
(23) $Li + D^+ \rightarrow Li^+ + D + v$	1.1E−13	−5.1E−2	282000	12
(24) $Li^+ + D^- \rightarrow Li + D$	2.06E−7	−0.50	−18300	11
(25) $Li + D^+ \rightarrow Li^+ + D$	8.0E−22	6.80	1800	13
(26) $Li^- + D^+ \rightarrow Li + D$	2.06E−7	−0.50	−18300	14
(27) $H + H^+ \rightarrow H_2^+ + v$	6.0E−19	1.8	−20[b]	15
(28) $H_2^+ + v \rightarrow H + H^+$	...	...	...	2
(29) $H^+ + H^- \rightarrow H_2^+ + e^-$	1.0E−9	−0.4	...	16
(30) $H_2^+ + e^- \rightarrow H + H$	1.2E−8	−0.4	...	17
(31) $H_2^+ + H \rightarrow H_2 + H^+$	6.4E−10	0	...	18
(32) $H_2^+ + H^- \rightarrow H_2 + H$	1.4E−7	−0.5	...	4
(33) $H_2^+ + H^- \rightarrow H + H + H$	1.4E−7	−0.5	...	4
(34) $H_2 + He^+ \rightarrow H_2^+ + He + v$	7.2E−15	0	...	19
(35) $H_2 + He^+ \rightarrow He + H + H^+$	3.7E−14	0	35[b]	19
(36) $H + H^- \rightarrow H_2 + e^-$	1.5E−9	−0.1	...	20
(37) $He + H^+ \rightarrow HeH^+ + v$	8.0E−20	−0.24	4000	21
(38) $He + H^+ + v_r \rightarrow HeH^+ + v + v_r$	1.5E−20	0	200[b]	22
(39) $HeH^+ + v \rightarrow He + H^+$	...	...	...	2
(40) $He^+ + H \rightarrow HeH^+ + v$	4.16E−16	−0.37	87600	23
(41) $HeH^+ + H \rightarrow H_2^+ + He$	1.04E−9	0.13	33100	24
(42) $He + H_2^+ \rightarrow HeH^+ + H$	3.0E−10	0	6720[b]	25
(43) $HeH^+ + e^- \rightarrow He + H$	3.0E−8	−0.47	...	26
(44) $H_2^+ + H_2 \rightarrow H_3^+ + H$	2.24E−9	4.2E−2	46600	24
(45) $HeH^+ + H_2 \rightarrow H_3^+ + He$	1.53E−9	0.24	14800	24
(46) $H_2 + H^+ \rightarrow H_3^+ + v$	1.0E−20	...	...	8
(47) $H_2^+ + H \rightarrow H_3^+ + v$	1.5E−17	1.8	−20[b]	8
(48) $H_3^+ + e^- \rightarrow H_2 + H$	4.0E−8	−0.5	...	27
(49) $H_3^+ + e^- \rightarrow H + H + H$	1.6E−7	−0.5	...	27
(50) $H_3^+ + H^- \rightarrow H_2 + H + H$	2.3E−7	−0.5	...	8
(51) $H + D^+ \rightarrow HD^+ + v$	3.9E−19	1.8	−20[b]	28
(52) $HD^+ + v \rightarrow H + D^+$	...	...	...	2
(53) $D + H^+ \rightarrow HD^+ + v$	3.9E−19	1.8	−20[b]	28
(54) $HD^+ + v \rightarrow D + H^+$	...	...	...	2
(55) $H_2^+ + D \rightarrow HD^+ + H$	1.07E−9	6.2E−2	41400	24
(56) $H_2^+ + D \rightarrow H_2 + D^+$	6.4E−10	0	...	6
(57) $HD^+ + e^- \rightarrow H + D$	3.4E−9	−0.4	...	29
(58) $HD^+ + H \rightarrow HD + H^+$	6.4E−10	0	...	6
(59) $HD^+ + H \rightarrow H_2^+ + D$	1.0E−9	0	154[b]	8
(60) $HD^+ + H_2 \rightarrow H_3^+ + D$	1.05E−9	0	...	5
(61) $H + D \rightarrow HD + v$	1.05E−26	0.09	7000	30
(62) $H + D + v_r \rightarrow HD + v + v_r$	2.0E−27	0	400[b]	30
(63) $H_2 + D^+ \rightarrow HD + H^+$	2.1E−9	0	...	31
(64) $HD + H^+ \rightarrow H_2 + D^+$	1.0E−9	0	457[b]	31
(65) $H_2 + D \rightarrow HD + H$	7.5E−11	0	3820[b]	32
(66) $HD + H \rightarrow H_2 + D$	7.5E−11	0	4240[b]	32
(67) $D + H^- \rightarrow HD + e^-$	1.5E−9	−0.1	...	7
(68) $D^- + H \rightarrow HD + e^-$	1.5E−9	−0.1	...	7
(69) $He^+ + D \rightarrow HeD^+ + v$	5.0E−16	−0.37	87600	7
(70) $He + D^+ \rightarrow HeD^+ + v$	1.0E−19	−0.24	4000	7
(71) $He + D^+ + v_r \rightarrow HeD^+ + v + v_r$	1.5E−21	0	200[b]	7
(72) $HeD^+ + v \rightarrow He + D^+$	...	...	...	2
(73) $HeH^+ + D \rightarrow HeD^+ + H$	1.0E−9	0	...	8

TABLE 1—*Continued*

Reaction	a_1 (cm^3 s^{-1})	a_2	a_3 (K)	Notes
(74) $HeD^+ + H \rightarrow HeH^+ + D$	8.0E$-$10	0	468[b]	8
(75) $HeD^+ + H \rightarrow HD^+ + He$	9.1E$-$10	0.13	33100	6
(76) $HeH^+ + D \rightarrow HD^+ + He$	8.5E$-$10	0.13	33100	6
(77) $HeD^+ + e^- \rightarrow He + D$	3.0E$-$8	-0.47	...	6
(78) $H_3^+ + HD \rightarrow H_2D^+ + H_2$	1.4E$-$9	0	...	31
(79) $H_2 + D^+ \rightarrow H_2D^+ + \nu$	1.0E$-$20	...	...	6
(80) $HD + H^+ \rightarrow H_2D^+ + \nu$	1.0E$-$20	...	...	6
(81) $H_2^+ + D \rightarrow H_2D^+ + \nu$	7.0E$-$18	1.8	-20[b]	6
(82) $HD^+ + H \rightarrow H_2D^+ + \nu$	1.2E$-$17	1.8	-20[b]	6
(83) $H_2D^+ + e^- \rightarrow H + H + D$	4.38E$-$8	-0.5	...	33
(84) $H_2D^+ + e^- \rightarrow H_2 + D$	4.2E$-$9	-0.5	...	33
(85) $H_2D^+ + e^- \rightarrow H + HD$	1.2E$-$8	-0.5	...	33
(86) $HD^+ + H_2 \rightarrow H_2D^+ + H$	1.05E$-$9	0	...	5
(87) $H_3^+ + D \rightarrow H_2D^+ + H$	1.0E$-$9	0	...	34
(88) $HD + H_2^+ \rightarrow H_2D^+ + H$	1.05E$-$9	0	...	35
(89) $HD + H_2^+ \rightarrow H_3^+ + D$	1.05E$-$9	0	...	35
(90) $H_2D^+ + H \rightarrow H_3^+ + D$	1.0E$-$9	0	632[b]	5
(91) $H_2D^+ + H_2 \rightarrow H_3^+ + HD$	1.7E$-$9	0	150[b]	31
(92) $HeD^+ + H_2 \rightarrow H_2D^+ + He$	1.24E$-$9	0.24	14800	6
(93) $HeH^+ + HD \rightarrow H_2D^+ + He$	1.20E$-$9	0.24	14800	6
(94) $He^+ + HD \rightarrow He + H^+ + D$	5.5E$-$14	-0.24	...	5
(95) $He^+ + HD \rightarrow He + H + D^+$	5.5E$-$14	-0.24	...	5
(96) $He + HD^+ \rightarrow HeH^+ + D$	3.0E$-$10	0	6720[b]	6
(97) $He + HD^+ \rightarrow HeD^+ + H$	3.0E$-$10	0	6720[b]	6
(98) $He + He^+ \rightarrow He_2^+ + \nu$	4.76E$-$20	1.82	-29[b]	36
(99) $He_2^+ + \nu \rightarrow He + He^+$	...	...	...	2
(100) $He_2^+ + e^- \rightarrow He + He$	5.0E$-$10	-0.5	...	37
(101) $He_2^+ + H \rightarrow He + He + H^+$	1.0E$-$9	0	...	38
(102) $LiH^+ + D \rightarrow Li + HD^+$	9.0E$-$10	...	66400[b]	39
(103) $LiH^+ + D \rightarrow Li^+ + HD$	3.0E$-$10	...	...	39
(104) $LiH^+ + D \rightarrow LiH + D^+$	1.0E$-$11	...	67900[b]	39
(105) $LiH + D^+ \rightarrow LiH^+ + D$	1.0E$-$9	...	...	39
(106) $LiH + D \rightarrow Li + HD$	2.0E$-$11	...	...	39
(107) $LiH + D^+ \rightarrow Li^+ + HD$	1.0E$-$9	...	...	39
(108) $LiH + D^+ \rightarrow Li + HD^+$	1.0E$-$9	...	...	39
(109) $H^* + H \rightarrow H_2^+ + e^-$	6.8E$-$12	0.61	13000[b]	40
(110) $H^* + H \rightarrow H_2 + \nu$	2.09E$-$14	0.24	37800	41
(111) $H^* + H_2 \rightarrow H_3^+ + e^-$	4.7E$-$9	-0.5	...	42
(112) $H^* + H_2 \rightarrow H + H + H$	2.5E$-$11	...	...	43
(113) $H^* + D \rightarrow HD^+ + e^-$	5.7E$-$12	0.61	13000[b]	7
(114) $D^* + H \rightarrow HD^+ + e^-$	5.7E$-$12	0.61	13000[b]	7
(115) $H^* + D \rightarrow HD + \nu$	2.0E$-$14	0.24	37800	7
(116) $D^* + H \rightarrow HD + \nu$	2.0E$-$14	0.24	37800	7
(117) $H^* + HD \rightarrow H_2D^+ + e^-$	5.4E$-$9	-0.5	...	7
(118) $D^* + H_2 \rightarrow H_2D^+ + e^-$	5.8E$-$9	-0.5	0	7
(119) $H^* + HD \rightarrow H + H + D$	2.5E$-$11	...	...	6
(120) $D^* + H_2 \rightarrow H + H + D$	2.5E$-$11	...	...	6

NOTE.—The rate coefficients fits are given by the relation $\alpha = a_1 (T/300)^{a_2} \exp(-T/a_3)$.

[a] The notation 3.6E$-$12 corresponds to 3.6×10^{-12}.

[b] For the indicated reactions the exponential term in the rate relation has the form $\exp(-a_3/T)$.

REFERENCES.—(1) Hollenbach & McKee 1989; (2) detailed balance applied to the reverse reaction; (3) determined by detailed balance from photodetachment cross section of Wishart 1979; (4) Dalgarno & Lepp 1987; (5) Pineau des Forêts et al. 1989; (6) same as corresponding H reaction; (7) same as corresponding H reaction but scaled by D reduced mass; (8) Dalgarno & McDowell 1956, but scaled by D reduced mass; (9) Pineau des Forêts et al. 1986; (10) Zygelman et al. 1989, multiplied by 0.25 to account for approach probability factor (see Stancil & Zygelman 1996); (11) determined from cross section of Peart & Hayton 1994; (12) Stancil & Zygelman 1996, but scaled by D reduced mass; (13) fitted to Kimura, Dutta, & Shimakura 1994, but scaled by D reduced mass; (14) assumed same as reaction (24); (15) fitted to Ramaker & Peek 1976; (16) Shapiro & Kang 1987; (17) fitted to Schneider et al. 1994, 1997; (18) Karpas et al. 1979; (19) Barlow 1994; (20) fitted to Launay, Le Dourneuf, & Zeippen 1991; (21) fitted to Juřek et al. 1995; (22) Zygelman et al. 1998; (23) fitted to Kraemer, Špirko, & Juřek 1995, multiplied by 0.25 to account for approach probability factor (see note 10); (24) determined from cross section of Linder, Janev, & Botero 1995; (25) Black 1978; (26) Guberman 1994; (27) Datz et al. 1995; (28) fitted to Ramaker & Peek 1976, but scaled by reduced mass, and Frommhold & Pickett 1978; (29) determined from cross section of Strömholm et al. 1995; (30) Stancil & Dalgarno 1997b; (31) Smith et al. 1982; (32) fitted to Zhang & Miller 1989; (33) Larsson et al. 1996; (34) Millar, Bennett, & Herbst 1989; (35) assumed same as reaction (80); (36) fitted to Stancil, Babb, & Dalgarno 1993; (37) estimated from Ivanov & Skoblo 1988; (38) estimate, Stancil et al. 1993; (39) same as corresponding H reaction estimate of Stancil et al. 1996; (40) fitted to Rawlings, Drew, & Barlow 1993 and Rawlings 1997, private communication; (41) fitted to Latter & Black 1991; (42) estimated from Dehmer & Chupka 1995; and (43) Geddes & McCullough 1994.

TABLE 2

COSMOLOGICAL MODEL PARAMETERS

Parameters	Model I	Model II	Model III	Model IV	Model V
Ω_0	1.0	1.0	1.0	1.0	0.3
Ω_b	0.1	1.0	0.0367	0.015	0.0367
h	0.5	0.5	0.67	0.67	0.67
$\Omega_b h^2$	0.025	0.25	0.0165	0.00673	0.0165
Y..........	0.284	0.263	0.242	0.230	0.242
n_{He}/n_H	0.1	9.0E$-$2	8.02E$-$2	7.5E$-$2	8.02E$-$2
n_D/n_H	5.0E$-$5	1.0E$-$4	4.0E$-$5	2.0E$-$4	4.0E$-$5
n_{Li}/n_H	1.0E$-$10	1.0E$-$8	2.3E$-$10	1.9E$-$10	2.3E$-$10

where Ω_b is the ratio of the baryonic-matter density to the critical density required to close the Universe, h is the Hubble constant in units of 100 km s^{-1} Mpc^{-1}, Y is the helium mass fraction, and the redshift z is related to the time by the expression

$$\frac{dt}{dz} = \frac{3.086 \times 10^{17}}{h(1+z)^2(1+\Omega_0 z)^{1/2}} \text{ s}^{-1} \qquad (23)$$

(e.g., Peebles 1993). The radiation temperature is given by $T_r = 2.728(1 + z)$ K (Fixsen et al. 1996). The matter temperature T_m is taken from the models of Puy et al. (1993). The H($n = 2$) abundances are taken from Rybicki & Dell'Antonio (1996), who made a careful study of the recombination epoch, including line-trapping of Lyα photons.

We have investigated five different cosmological models. Their parameters are given in Table 2, and all but Model V incorporate the closure parameter $\Omega_0 = 1.0$. Models I, II, and III are the same as described in Stancil et al. (1996). Model IV is the D-rich model used by Palla et al. (1995) corresponding to the assumed deuterium abundance along the line of sight to the high-redshift ($z = 3.32$) absorption complex toward quasar Q0014+813 (Songaila et al. 1994;

Rugers & Hogan 1996). Model V is an open universe model with $\Omega_0 = 0.3$ but with all other parameters identical to Model III. While Models I, II, and IV lie outside of the observationally deduced range of the baryonic fraction of the critical density, $0.009 \leq \Omega_b h^2 \leq 0.02$ (Copi, Schramm, & Turner 1995), we include them for comparison with previous chemical models.

4. RESULTS AND DISCUSSION

We determined the fractional abundances of all species listed in Table 3 as a function of redshift for the five different cosmological models. The results for our standard Model III are presented in Figures 1 and 2, while the fractional abundances at $z = 10$ for each of the models are given in Table 3 with a comparison to previous calculations. To visualize the primary reaction processes, Figures 3–12 plot the formation and destruction rates (with fractional abundances) for each of the molecules for Model III except He$_2^+$. Similar plots have been given by Abel et al. (1997) for H$^-$, H$_2^+$, and H$_2$ and by Bougleux & Galli (1997) for LiH.

As shown in Figure 3, HeH$^+$ is primarily formed by the radiative association reactions (T1.37) and (T1.38) with some contribution from (T1.42) peaking near $z \sim 300$. The

TABLE 3

FRACTIONAL ABUNDANCES $n(x)/n_H$ AT $z = 10$ FOR MODELS I–V

Species	I[a]	I[b]	I[c]	II[b]	II[c]	III[d]	III[c]	IV[e]	IV[c]	V[c]
H	...	...	0.9998	...	0.99997	0.9997	0.9996	0.9981	0.9992	0.9997
H$^+$, e$^-$	...	...	2.1E$-$4	...	2.5E$-$5	3.1E$-$4	4.0E$-$4	1.9E$-$3	7.6E$-$3	2.2E$-$4
H$^-$	<1E$-$11	...	4.0E$-$13	...	3.2E$-$14	3.2E$-$13	7.4E$-$13	...	8.5E$-$13	4.3E$-$13
D	...	...	5.0E$-$5	...	1.0E$-$4	4.3E$-$5	4.0E$-$5	...	2.0E$-$4	4.0E$-$5
D$^+$	...	...	1.6E$-$13	...	1.2E$-$16	0.0	2.4E$-$13	...	7.3E$-$15	1.3E$-$13
D$^-$	...	...	2.0E$-$17	...	3.2E$-$18	...	2.9E$-$17	...	1.7E$-$16	1.7E$-$17
He............	...	...	1.0E$-$1	...	9.0E$-$2	8.0E$-$2	8.04E$-$2	...	7.5E$-$2	8.04E$-$2
He$^+$	...	...	2.7E$-$26	...	2.5E$-$31	2.6E$-$24	1.8E$-$24	...	5.5E$-$23	2.8E$-$26
Li............	...	...	5.5E$-$11	...	9.1E$-$9	1.0E$-$10	1.2E$-$10	...	1.1E$-$10	1.2E$-$10
Li$^+$	...	...	4.5E$-$11	...	9.3E$-$10	1.3E$-$10	1.1E$-$10	...	7.7E$-$11	1.1E$-$10
Li$^-$	...	...	4.5E$-$22	...	9.5E$-$21	1.8E$-$21	1.4E$-$21	...	9.4E$-$22	1.1E$-$21
H$_2^+$	<1E$-$12	...	2.4E$-$14	...	1.6E$-$14	2.0E$-$13	4.2E$-$14	1.9E$-$12	4.4E$-$13	2.4E$-$14
H$_2$............	1.2E$-$6	8.5E$-$6	2.5E$-$6	8.5E$-$6	4.6E$-$6	1.1E$-$6	2.4E$-$6	5.3E$-$6	1.1E$-$6	2.4E$-$6
HeH$^+$	4.0E$-$14	...	7.6E$-$15	...	1.0E$-$15	1.4E$-$13	1.1E$-$14	...	1.9E$-$14	6.5E$-$15
He$_2^+$	...	...	1.1E$-$37	...	2.5E$-$41	...	6.1E$-$36	...	4.6E$-$33	9.1E$-$38
H$_3^+$	...	...	2.5E$-$19	...	1.9E$-$18	4.0E$-$17	2.1E$-$19	...	3.9E$-$19	2.2E$-$19
LiH	1.8E$-$13	6.0E$-$11	7.0E$-$20	6.0E$-$10	1.0E$-$17	1.4E$-$19	1.6E$-$19	1.9E$-$13	1.3E$-$19	1.6E$-$19
LiH$^+$	...	...	9.4E$-$19	...	2.6E$-$17	3.1E$-$18	3.6E$-$18	3.8E$-$18	6.0E$-$18	2.3E$-$18
HD$^+$	...	...	2.8E$-$18	...	3.2E$-$18	6.7E$-$19	3.8E$-$18	1.4E$-$21	1.7E$-$16	2.2E$-$18
HD	6.0E$-$11	7.0E$-$9	2.2E$-$9	5.1E$-$8	1.8E$-$8	1.1E$-$9	1.6E$-$9	3.0E$-$8	3.0E$-$9	1.7E$-$9
HeD$^+$	...	...	6.7E$-$19	...	2.1E$-$19	...	7.1E$-$19	...	5.3E$-$18	4.6E$-$19
H$_2$D$^+$	...	...	7.7E$-$22	...	3.0E$-$20	7.5E$-$20	4.8E$-$22	1.4E$-$16	3.3E$-$21	5.3E$-$22

[a] Lepp & Shull (1984).
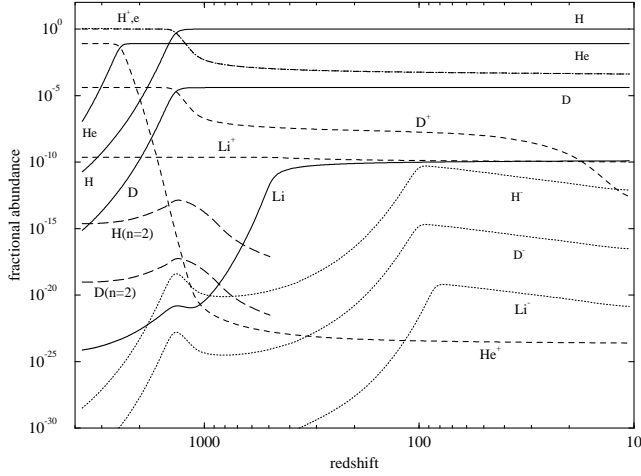[b] Puy et al. (1993).
[c] This work.
[d] GP.
[e] Palla et al. (1995).

FIG. 1.—Fractional abundances $n(x)/n_H$ of atoms for the Model III chemistry of the recombination era primordial gas. $\Omega_b h^2 = 0.0165$, $Y = 0.242$, $n_{He}/n_H = 0.0802$, $n_D/n_H = 4.0 \times 10^{-5}$, $n_{Li}/n_H = 2.3 \times 10^{-10}$ (see Table 2 for other parameters).
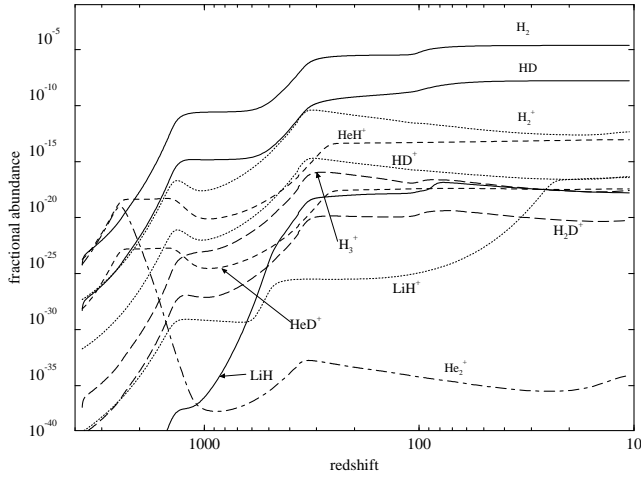

FIG. 2.—Fractional abundances of molecules for the Model III chemistry of the recombination era primordial gas (see Table 2 for parameters).
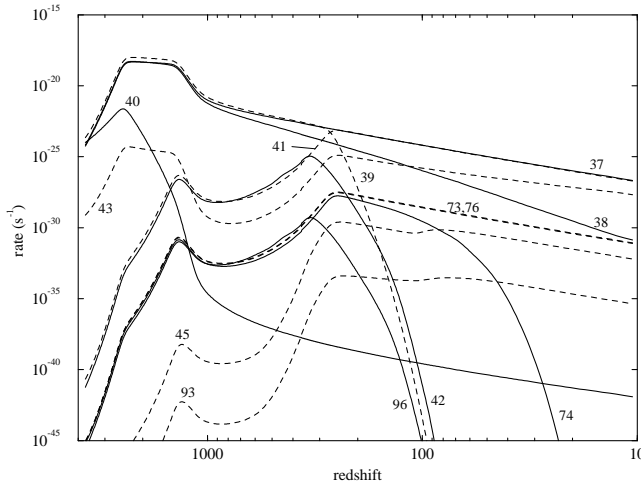

FIG. 3.—Rates of dominant HeH^+ formation (*solid lines*) and destruction (*dotted lines*) processes for Model III. The numbers correspond to the reactions listed in Table 1.
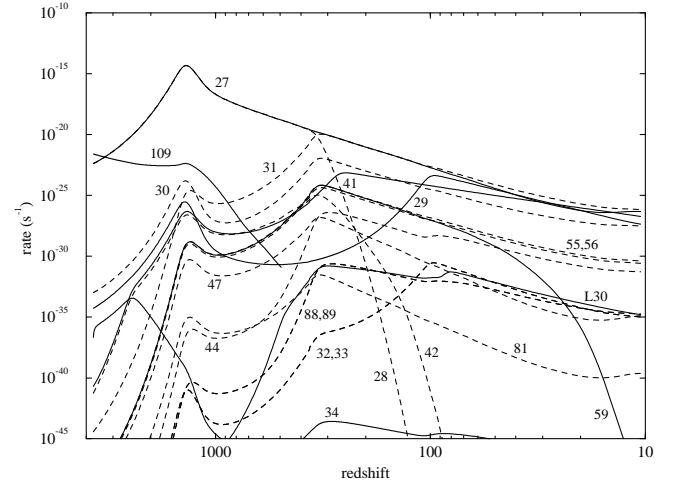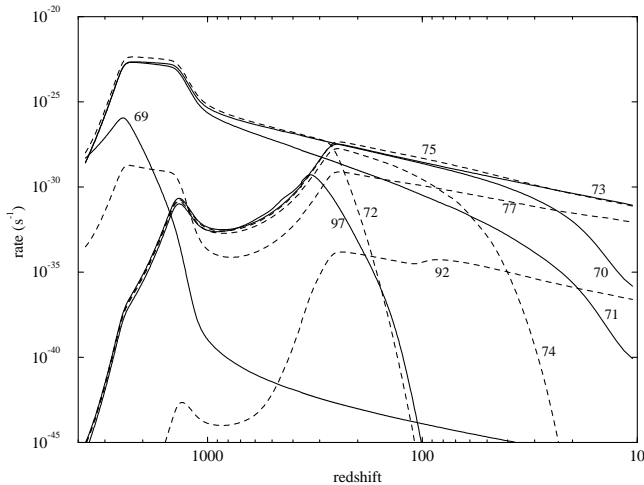

FIG. 4.—Same as Fig. 3 but for H_2^+

radiative association reaction (T1.40) is only important for $z > 3000$ when there is significant He^+ abundance. HeH^+ is mainly destroyed by photodissociation (T1.39) for $z \gtrsim 300$ and by collisions with H (T1.41) and dissociative recombination (T1.43) for $z \lesssim 300$. The remaining reactions play only minor roles in the chemistry. The HeH^+ chemistry is similar to that used by GP. However, GP adopted the inverse predissociation rate coefficients of Roberge & Dalgarno (1982) for (T1.37), which are an order of magnitude larger than the results of Jurek, Špirko, & Kraemer (1995). The Jurek et al. (1995) results have been confirmed by Zygelman et al. (1998). This discrepancy is reflected in the HeH^+ fractional abundance given in Table 3. With the exception of (T1.37), the major uncertainty in the HeH^+ reaction network is (T1.41). The adopted rate coefficient is limited to the ion cyclotron resonance measurement of Karpas, Anicich, & Huntress (1979). Additional studies of (T1.41), including its vibrational state dependence, are needed.

The formation and destruction processes of H_2^+ are shown in Figure 4. After recombination it is primarily produced by radiative association (T1.27); earlier it is made by associative detachment of H with H($n = 2$) (T1.109). For $z \lesssim 100$, (T1.29) and proton abstraction from HeH^+ (T1.41) contribute significantly and dominate (T1.27) for $z \lesssim 40$. For $z \gtrsim 400$, photodissociation (T1.28) is the primary destruction mechanism, but at later times H_2^+ is mainly removed by charge exchange with H (T1.31). Dissociative recombination (T1.30) is also a significant destruction path for $z \lesssim 400$. Even though GP adopted a similar chemistry, our H_2^+ abundance is nearly a factor of 5 smaller, as shown in Table 3 at $z = 10$. This discrepancy is related to their larger HeH^+ abundance, since (T1.41) becomes their dominant H_2^+ production mode at late times. In addition to (T1.41), the primary uncertainty in the H_2^+ chemical network is the adopted rate coefficient for (T1.31), which, as is the case for (T1.41), is taken from the measurement of Karpas et al. (1979).

Figure 5 shows that H_2 is formed through H_2^+ by (T1.31) for $130 \lesssim z \lesssim 700$ and through H^- by (T1.36) for $z \lesssim 130$. Some contributions are made through deuterated species by (T1.64) and (T1.66), and as noted by Latter & Black (1991), reaction (T1.110) with excited H forms some H_2 for $z \gtrsim 1300$; however, its abundance is kept low because of the
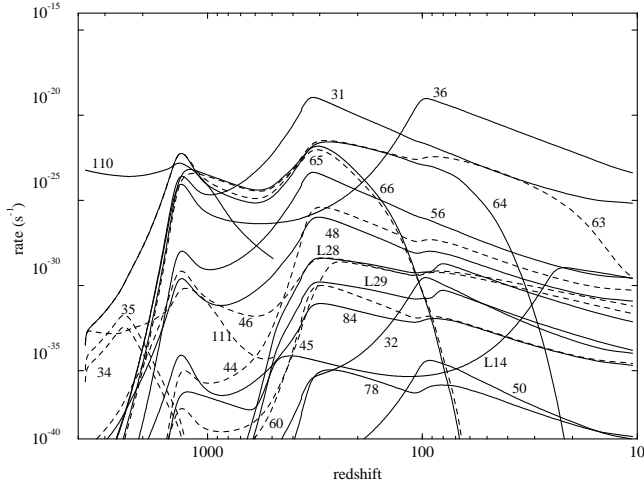
FIG. 5.—Same as Fig. 3 but for H_2
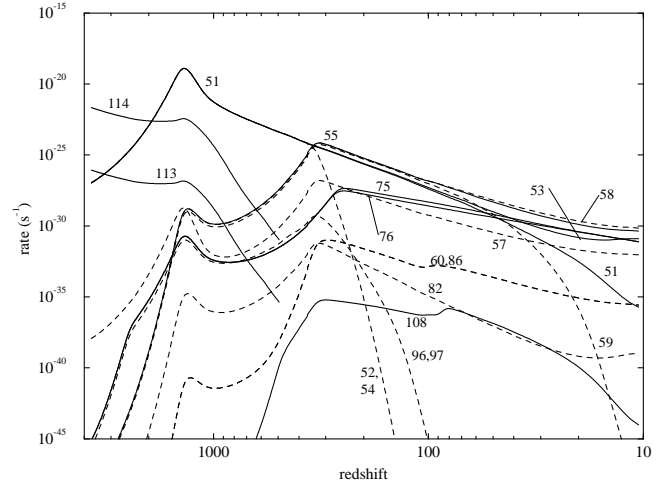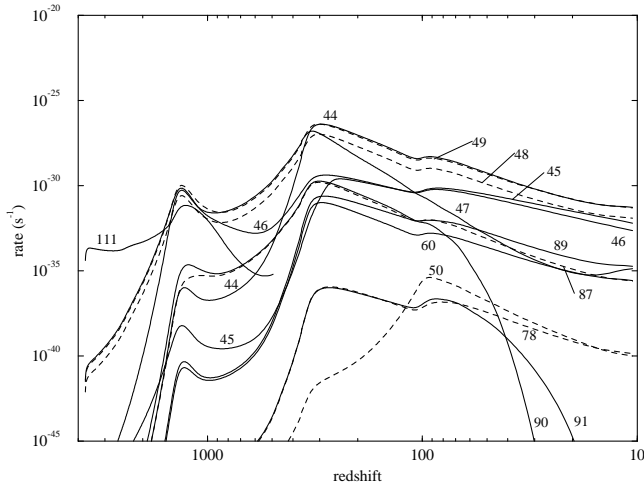
FIG. 6.—Same as Fig. 3 but for H_3^+

FIG. 7.—Same as Fig. 3 but for HeD^+

FIG. 8.—Same as Fig. 3 but for HD^+

high efficiency of H photoionization (T1.2). H_2 is robust and, because the CBR lacks a consequential UV component, suffers from no significant destruction processes. Only collisions with D^+ (T1.63) and D (T1.65) and, for $z \gtrsim 2000$, collisions with He^+ (T1.34) and (T1.35) are effective. Our computed abundance is in good agreement with GP at $z = 10$, since the adopted chemistries are nearly identical. As for H_2^+, the primary uncertainty is the reliability of the measured rate coefficient for (T1.31).

The most abundant polyatomic molecule formed in the early universe is H_3^+, and its important reaction rates are displayed in Figure 6. As in interstellar clouds (Martin, McDaniel, & Meeks 1961; Herbst & Klemperer 1973), it is primarily produced by (T1.44), but for $z \gtrsim 1500$ the excited H reaction (T1.111) is the major formation route. (T1.45) and (T1.89) make minor contributions. At all redshifts, H_3^+ is primarily destroyed by dissociative recombination (T1.49) and (T1.48). Our abundance estimate is more than 2 orders of magnitude smaller than that obtained by GP. The chemistry is comparable, except that GP primarily produce H_3^+ by the radiative association reaction (T1.46). For (T1.46) they adopted the large rate coefficient 1×10^{-16} cm³ s⁻¹ recommended by Gerlich & Horning (1992) based on an ion trap measurement and a classical trajectory analysis. However, the reaction involves rovibrational transitions within the ground electronic state, and experience from fully quantal calculations for diatomic systems such as HeH^+, LiH^+, and LiH suggests that the rate coefficient should be much smaller. We prefer the temperature-independent value of 1×10^{-20} cm³ s⁻¹. Reaction (T1.46) needs to be further investigated before an accurate picture of H_3^+ can be obtained.

As shown in Figure 7, the primary reactions involved in the chemistry of HeD^+ are similar to those for HeH^+. It is produced by radiative association (T1.70) and the exchange reaction (T1.97), and it is destroyed by photodissociation (T1.72) and the exchange reaction (T1.75). Additionally, the D exchange reaction (T1.73) is an important HeD^+ production mechanism. The abundance of HeD^+ tracks that of HeH^+. The chemistry is rather uncertain, because all of the adopted rate coefficients are taken from corresponding He–H reactions but scaled by the collision system reduced mass. Similar to HeH^+, the most uncertain reaction is that of (T1.75). No previous abundance estimates of HeD^+ have been reported. We did not consider ³He since its chemistry
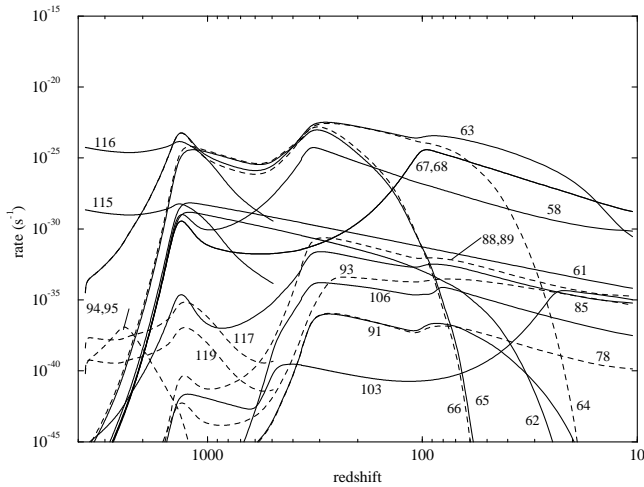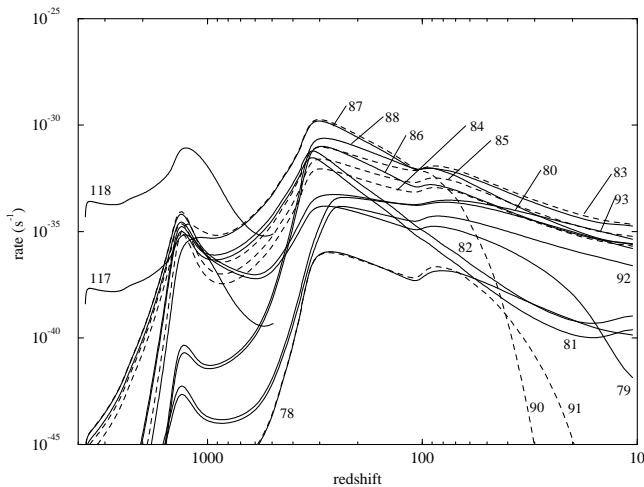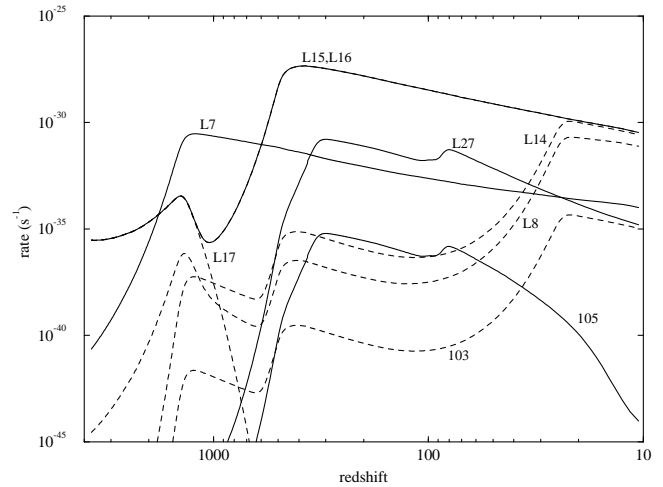
FIG. 9.—Same as Fig. 3 but for HD

FIG. 11.—Same as Fig. 3 but for LiH$^+$

is not expected to be different from that of ^{4}He. The He reaction analogous to (T1.8) (Dutta, Lane, & Kimura 1992) is unimportant, since the He$^+$ abundance is negligible for $z < 1000$.

Figure 8 shows that the reaction network for HD$^+$ is comparable to that of H$_2^+$. It is produced by the radiative association processes (T1.51) and (T1.53), D$^+$ abstraction from HeD$^+$ (T1.75), and proton abstraction from HeH$^+$ (T1.76). HD$^+$ is removed by photodissociation (T1.52) and (T1.54) for $z \gtrsim 400$ and by charge exchange (T1.58) and dissociative recombination (T1.57) for $z \lesssim 400$. However, the exchange reaction (T1.55), for which there is no comparable process in the H$_2^+$ formation scheme, becomes the dominant formation mechanism for $z \lesssim 400$. Our computed HD$^+$ abundance is larger than that of GP, since they neglected (T1.55), (T1.75), and (T1.76). Most of the chemistry is uncertain, because only dissociative recombination (T1.57) has been explicitly investigated, while the remaining reaction rates were deduced from the corresponding hydrogen chemistry. Further studies of (T1.55) and (T1.58) are of most importance.

Similar to H$_2$, HD is produced by associative detachment (T1.67) and (T1.68) for $z \lesssim 130$, charge exchange (T1.58) for $130 \lesssim z \lesssim 600$, and excited H reactions (T1.115) and (T1.116) for $z \gtrsim 1000$, as shown in Figure 9. However, the

primary HD formation process is actually the D exchange reactions (T1.63) and (T1.65) with the reverse D exchange reactions (T1.64) and (T1.66) being the dominant destruction routes. Quite good agreement is found between the current abundance estimates and that obtained by GP. The adopted rate coefficients of (T1.63) and (T1.64) are from the flow-tube measurements of Smith, Adams, & Alge (1982), while those of (T1.65) and (T1.66) are based on the calculations of Zhang & Miller (1989). Further studies are needed to reduce the uncertainty in the HD abundance.

H$_2$D$^+$ is formed by (T1.88) and (T1.86) for $z \lesssim 1000$, (T1.93) for $z \lesssim 20$, and (T1.117) and (T1.118) for $z \gtrsim 1000$. It is destroyed by dissociative recombination (T1.83)–(T1.85). However, unlike H$_3^+$, (T1.87) and (T1.90) are the primary formation and destruction mechanisms for $130 \lesssim z \lesssim 1000$, as displayed in Figure 10. The discrepancy with the abundance estimates of GP is a consequence of their enhanced H$_3^+$ abundance. The other major uncertainties in the H$_2$D$^+$ chemistry are due to the limited information on (T1.87), (T1.88), and (T1.90).

For completeness, we also show in Figures 11 and 12 the primary formation and destruction processes for LiH$^+$ and LiH, respectively. LiH$^+$ is primarily formed by the radiative

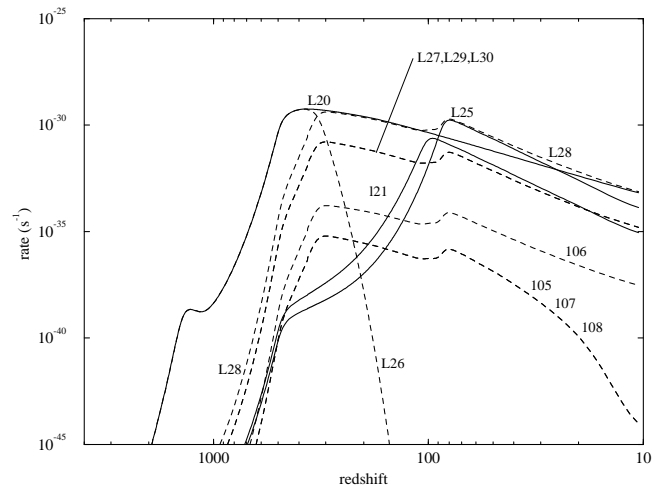FIG. 10.—Same as Fig. 3 but for H$_2$D$^+$

FIG. 12.—Same as Fig. 3 but for LiH

TABLE 4

DEUTERIUM FRACTIONATION AT $z = 10$ FOR MODELS I–V

Species	I[a]	I[b]	I[c]	II[b]	II[c]	III[d]	III[c]	IV[e]	IV[c]	V[c]
D/H	5.0E−5	1.7E−5	5.0E−5	1.0E−4	1.0E−4	4.3E−5	4.0E−5	2.0E−4	2.0E−4	4.0E−5
D^+/H^+	...	...	7.5E−10	...	4.8E−12	0	6.0E−10	...	9.6E−12	6.0E−10
D^-/H^-	...	...	5.0E−5	...	1.0E−4	...	4.0E−5	...	2.0E−4	4.0E−5
$HD^+H_2^+$	...	...	1.2E−4	...	2.0E−4	3.3E−6	9.1E−5	7.4E−10	3.9E−4	9.3E−5
HD/H_2	5.0E−5	8.2E−4	8.9E−5	6.0E−3	3.8E−3	1.0E−3	6.9E−4	5.7E−3	2.8E−3	7.0E−4
HeD^+/HeH^+	...	...	8.9E−5	...	2.0E−4	...	6.6E−5	...	2.8E−4	7.1E−5
H_2D^+/H_3^+	...	...	3.1E−3	...	1.6E−2	1.9E−3	2.2E−3	5.2E−3	8.6E−3	2.4E−3

[a] Lepp & Shull (1984).
[b] Puy et al. (1993).
[c] This work.
[d] GP.
[e] Palla et al. (1995).

association reactions (L7)[7] and (L15) and destroyed by photodissociation (L16) and (L17). However, for $z \lesssim 25$, the exchange reaction (L14) and dissociative recombination (L8) are the important destruction mechanisms. Radiative association (L20) and associative detachment (L25) are the main production mechanisms for LiH, while photodissociation (L26) and collisions with H (L28) are the dominant removal routes. The current abundances of LiH⁺ and LiH are in good agreement with GP. GP also include LiH formation from excited Li radiative association, but Bougleux & Galli (1997) have shown that it only contributes for $z \gtrsim 650$. Reactions (L28), (L25), (L14), and (L8) are the major uncertainties.

We have run other cosmological models for comparison with previous calculations. The current H_2 abundance is in good agreement with the results of Lepp & Shull (1984) for Model I but is nearly a factor of 4 smaller than Puy et al. (1993). The Lepp & Shull HD abundance appears to be too small, while that of Puy et al. is too large. Both previous calculations found erroneously large LiH abundances because of the adoption of a large radiative association rate coefficient.

For the baryonic ($\Omega_b = 1$) universe model II, our H_2, HD, and LiH abundances are smaller than those obtained by Puy et al. (1993), but larger than any of our other models mostly as a consequence of a higher density and enhanced D and Li primordial abundances. The cause of the large LiH discrepancy is the same as discussed for Model I. As noted by Palla et al. (1995), the enhanced D model (Model IV) has little effect on H_2 but increases the deuterium species abundances: HD⁺, HeD⁺, HD, and H_2D^+. The open universe Model V results in a slightly reduced ionization fraction due to the increase in time per unit redshift (see eq. [23]) as compared to Model III. The abundances of all the ions are decreased except for Li⁺, H_3^+, and H_2D^+.

Table 4 presents the deuterium fractionation. For Model III we find the isotope abundance ratios $n(HD^+)/n(H_2^+)$, $n(HD)/n(H_2)$, and $n(H_2D^+)/n(H_3^+)$ to be enhanced compared to the primordial abundance ratio $n_D/n_H = 4 \times 10^{-5}$ by factors of up to ~ 50. Conversely, the $n(D^+)/n(H^+)$ ratio is reduced by a factor of about 10^5, since for $z < 40$, D⁺ is significantly depleted because of the charge transfer reaction (T1.9). The reverse reaction (T1.8) is endothermic by 41 K. Comparing to GP, the ratios $n(HD)/n(H_2)$ and

$n(H_2D^+)/n(H_3^+)$ are in fair agreement, but the HD⁺ discrepancy persists for $n(HD^+)/n(H_2^+)$.

The enhanced HD/H_2 fractionation can be attributed to reactions (T1.63) and (T1.65). The endothermicity of reaction (T1.90) with respect to (T1.87) and the smaller rate coefficients of (T1.83)–(T1.85) compared to dissociative recombination of H_3^+ account for the H_2D^+/H_3^+ fractionation. While reactions (T1.78) and (T1.91) are important deuterium fractionation mechanisms in interstellar clouds (Dalgarno & Lepp 1984), they are negligible here; the reactions may play a role in collapsing primordial clouds.

5. IMPLICATIONS FOR CBR ANISOTROPIES

Dubrovich (1993) has suggested that Thomson scattering of CBR photons with H_2D^+ in early epochs might provide for suppression of spatial anisotropies in the CBR spectrum. He inferred that the H_2D^+ opacity may be near unity since it can be formed through reaction (T1.78), leading to significant fractionation $n(H_2D^+)/n(H_3^+)$ much greater than the primordial deuterium abundance. We find that while the fractionation is about 50, the abundances of both H_3^+ and H_2D^+ are small. It was previously pointed out by Palla et al. (1995) that the H_2D^+ optical depth is $< 10^{-9}$ and therefore would have a negligible effect on the CBR spectrum. Our H_2D^+ abundance is much smaller than that obtained by Palla et al., suggesting an optical depth of $\lesssim 10^{-14}$ but confirming their conclusion. We also note that (T1.78) plays an insignificant role in H_2D^+ production in the early universe, as shown in Figure 10.

Dubrovich & Lipovka (1995) have investigated the effect of H_2D^+ on distortions of the CBR spectrum for $z = 10–30$. The detection of these features could be used to determine the epochs of reionization and reheating ($z \sim 7$ and 10, respectively; e.g., Gnedin & Ostriker 1997) and could possibly place constraints on the primordial deuterium abundance. Assuming an H_2D^+ fractional abundance of 10^{-8}, Dubrovich & Lipovka (1995) obtained intensity contrasts in the Rayleigh-Jeans region of the CBR of $< 10^{-7}$. Since the intensity contrast scales linearly with abundance, the present calculations suggest H_2D^+ had an insignificant effect on the CBR distortions, precluding the possibility of obtaining any interesting cosmological information.

6. CONCLUSIONS

In conjunction with our previous investigation of the lithium chemistry, a comprehensive survey of all the relevant reactions in the recombination era of the early universe

---

[7] The reaction labels (Lx) in the figures correspond to process (x) in Stancil et al. (1996), where the lithium chemistry was fully discussed.

for the primordial elements has been performed. The computed abundances of 23 atomic and molecular species for a standard Big Bang cosmogony are generally in good agreement with the recent calculation of GP. However, because of some differences in the adopted rate coefficients, discrepancies remain for the less abundant molecular ions H_2^+, HeH^+, H_3^+, HD^+, and H_2D^+. To resolve these discrepancies, additional studies of reactions (T1.41), (T1.46), (T1.55), (T1.58), (T1.64), (T1.66), (T1.87), (T1.88), and (T1.90) are necessary.

For H_2, uncertainty remains in its formation because of limited information on the charge exchange reaction (T1.31) at low energies. Additional investigations of the D exchange reactions (T1.63) and (T1.65), the primary formation mechanisms of HD, are needed. Because H_2 and HD are predicted

to be the most abundant molecules, an accurate determination of their abundances in the postrecombination era is vital. They are expected to be the dominant coolants in the collapse of the first bound objects (Palla, Salpeter, & Stahler 1983; Lepp & Shull 1984).

REFERENCES

Abel, T., Anninos, P., Zhang, Y., & Norman, M. L. 1997, NewA, 2, 181
Barlow, S. G. 1984, Ph.D. thesis, Univ. Colorado
Black, J. H. 1978, ApJ, 222, 125
Bougleux, E., & Galli, D. 1997, MNRAS, 288, 638
Burles, S., & Tytler, D. 1996, AJ, 114, 1330
Carswell, R. F., Rauch, M., Weymann, R. J., Cooke, A. J., & Webb, J. K. 1994, MNRAS, 268, L1
Carswell, R. F., et al. 1996, MNRAS, 278, 518
Copi, C. J., Schramm, D. N., & Turner, M. S. 1995, Science, 267, 192
Dalgarno, A., & Fox, J. L. 1994, in Unimolecular and Bimolecular Reaction Dynamics, ed. C. Y. Ng, T. Baer, & I. Powis (Chichester: Wiley), 1
Dalgarno, A., & Lepp, S. 1984, ApJ, 287, L47
———. 1987, in Astrochemistry, ed. S. P. Tarafdar & M. P. Varshni (Dordrecht: Reidel), 109
Dalgarno, A., & McDowell, M. R. C. 1956, Proc. Phys. Soc. London A, 69, 615
Dalgarno, A., Weisheit, J. C., & Black, J. H. 1973, Astrophys. Lett., 14, 77
Datz, S., et al. 1995, Phys. Rev. Lett., 74, 876
Dehmer, P. M., & Chupka, W. A. 1995, J. Phys. Chem., 99, 1686
Dubrovich, V. K. 1993, Astron. Lett., 19, 53
Dubrovich, V. K., & Lipovka, A. A. 1995, A&A, 296, 301
Dutta, C. M., Lane, N. F., & Kimura, M. 1992, Phys. Rev. A, 46, 3889
Fixsen, D. J., Cheng, E. S., Gales, J. M., Mather, J. C., Shafer, R. A., & Wright, E. L. 1996, ApJ, 473, 576
Frommhold, L., & Pickett, H. M. 1978, Chem. Phys., 28, 441
Galli, D., & Palla, F. 1998, A&A, 335, 403
Gaur, V. P., & Tripathi, B. M. 1985, J. Quant. Spectrosc. Radiat. Transfer, 33, 291
Geddes, J., & McCullough, R. W. 1993, J. Phys. B, 26, L165
Gerlich, D., & Horning, S. 1992, Chem. Rev., 92, 1509
Gnedin, N. Y., & Ostriker, J. 1997, ApJ, 486, 581
Guberman, S. L. 1994, Phys. Rev. A, 49, R4277
Herbst, E., & Klemperer, W. 1973, ApJ, 185, 505
Hollenbach, D., & McKee, C. F. 1989, ApJ, 342, 306
Irwin, A. W. 1981, ApJS, 45, 624
Ivanov, V. A., & Skoblo, Yu. E. 1988, Opt. Spectrosc., 65, 445
Jurek, M., Špirko, V., & Kraemer, W. P. 1995, Chem. Phys., 193, 287
Karpas, Z., Anicich, V., & Huntress, W. T. 1979, J. Chem. Phys., 70, 2877
Kimura, M., Dutta, C. M., & Shimakura, N. 1994, ApJ, 430, 435
Kraemer, W. P., Špirko, V., & Jurek, M. 1995, Chem. Phys. Lett., 236, 177
Larsson, M., et al. 1996, A&A, 309, L1
Latter, W. B. 1989, Ph. D. thesis, Univ. Arizona
Latter, W. B., & Black, J. H. 1991, ApJ, 372, 161
Launay, J. M., Le Dourneuf, M., & Zeippen, C. J. 1991, A&A, 252, 842

Lepp, S., & Shull, J. M. 1984, ApJ, 280, 465
Linder, F., Janev, R. K., & Botero, J. 1995, in Atomic and Molecular Processes in Fusion Edge Plasmas, ed. R. K. Janev (New York: Plenum Press), 397
Martin, D. W., McDaniel, E. W., & Meeks, M. L. 1961, ApJ, 134, 1012
Millar, T. J., Bennett, A., & Herbst, E. 1989, ApJ, 340, 906
Palla, F., Galli, D., & Silk, J. 1995, ApJ, 451, 44
Palla, F., Salpeter, E. E., & Stahler, S. W. 1983, ApJ, 271, 632
Peart, B., & Hayton, D. A. 1994, J. Phys. B, 27, 2551
Peebles, P. J. E. 1993, Principles of Physical Cosmology (Princeton: Princeton Univ. Press)
Pineau des Forêts, G., Flower, D. R., Hartquist, T. W., & Dalgarno, A. 1986, MNRAS, 220, 801
Pineau des Forêts, G., Roueff, E., & Flower, D. R. 1989, MNRAS, 240, 167
Puy, D., Alecian, G., Le Bourlot, J., Léorat, J., & Pineau des Forêts, G. 1993, A&A, 267, 337
Ramaker, D. E., & Peek, J. M. 1976, Phys. Rev. A, 13, 58
Rawlings, J. M. C., Drew, J. E., & Barlow, M. J. 1993, MNRAS, 265, 968
Roberge, W., & Dalgarno, A. 1982, ApJ, 255, 489
Rodgers, S. D., & Millar, T. J. 1996, MNRAS, 280, 1046
Rugers, M., & Hogan, C. J. 1996, ApJ, 459, L1
Rybicki, G. B., & Dell'Antonio, I. P. 1996, BAAS, 188, 3202
Sauval, A. J., & Tatum, J. B. 1984, ApJS, 56, 193
Schneider, I. F., Dulieu, O., Giusti-Suzor, A., & Roueff, E. 1994, ApJ, 424, 983
———. 1997, ApJ, 486, 580
Shapiro, P. R., & Kang, H. 1987, ApJ, 318, 32
Smith, D., Adams, N. G., & Alge, E. 1982, ApJ, 263, 123
Songaila, A., Cowie, L. L., Hogan, C. J., & Rugers, M. 1994, Nature, 368, 599
Stancil, P. C., Babb, J. F., & Dalgarno, A. 1993, ApJ, 414, 672
Stancil, P. C., & Dalgarno, A. 1997a, ApJ, 479, 543
———. 1997b, ApJ, 490, 76
———. 1998, Faraday Disc., 109, 61
Stancil, P. C., Lepp, S., & Dalgarno, A. 1996, ApJ, 458, 401
Stancil, P. C., & Zygelman, B. 1996, ApJ, 472, 102
Strömholm, C., et al. 1995, Phys. Rev. A, 52, R4320
Tytler, D., Fan, X.-M., & Burles, S. 1996, Nature, 381, 207
Wishart, A. W. 1979, MNRAS, 187, 59
Zhang, J. Z. H., & Miller, W. H. 1989, J. Chem. Phys., 91, 1528
Zygelman, B., Dalgarno, A., Kimura, M., & Lane, N. F. 1989, Phys. Rev. A, 40, 2340
Zygelman, B., Stancil, P. C., & Dalgarno, A. 1998, ApJ, 508, 151